Determination of the astrophysical S factor of the ^{8}B(p,γ)^{9}C capture reaction from the d(^{8}B,^{9}C)n reaction

D. Beaumel [a,b], T. Kubo [a], T. Teranishi [a], H. Sakurai [a], S. Fortier [b], A. Mengoni [a,c], N. Aoi [a], N. Fukuda [a], M. Hirai [a], N. Imai [a], H. Iwasaki [a], H. Kumagai [a], H. Laurent [b], S.M. Lukyanov [a,d], J.M. Maison [b], T. Motobayashi [e], T. Nakamura [g], H. Ohnuma [f], S. Pita [b], K. Yoneda [a], M. Ishihara [a,g],

[a] *RIKEN(The Institute of Physical and Chemical Research), 2-1 Hirosawa, Wako, Saitama 351-0198, Japan*

[b] *Institut de Physique Nucléaire, IN2P3-CNRS, 91406 Orsay Cedex,France*

[c] *ENEA, I-40138 Bologna, Italy*

[d] *Flerov Laboratory of Nuclear Reactions, Joint Institute for Nuclear Research 141980 Dubna, Moscow region, Russia*

[e] *Department of Physics, Rikkyo University, Toshima-ku, Tokyo 171, Japan*

[f] *Department of Physics, Chiba Institute of Technology, Chiba 275-0023, Japan*

[g] *Department of Physics, University of Tokyo, 7-3-1 Hongo, Bunkyo, Tokyo 113, Japan*

Abstract

The asymptotic normalization coefficients for the virtual decay ^{9}C $\rightarrow$ ^{8}B + p have been determined by measuring the cross-section of the ^{8}B(d,n)^{9}C reaction in inverse kinematics at 14.4 MeV/u, using the RIPS facility. The deduced astrophysical S factor S_{18} of the ^{8}B(p,γ)^{9}C capture reaction in the center of mass energy range 1-100 keV is $S_{18} = 45 \pm 13 eV.b$.

Key words: Transfer reactions with radioactive nuclear beams, DWBA analysis, Asymptotic Normalization Coefficients, astrophysical S factor
PACS: 25.60.Je, 25.40.Lw, 26.30.+k

1 Introduction

Radiative capture such as (p,γ) reactions are of crucial interest in astrophysics, since they play an important part in basic processes such as hydrogen burning. The thermonuclear energies relevant for such astrophysical processes are well below the Coulomb barrier, typically where cross-sections are very small. The measurement of such cross-sections is even more complicated when short-lived radioactive nuclides are involved in the entrance channel. This has lead to the implementation of indirect methods allowing the experimental difficulties inherent to the direct measurements of capture cross-section to be circumvented.

A few years ago, such an indirect approach based on measurements of *peripheral proton transfer* cross-sections on ^{7}Be was proposed [1,2] as yet another way to determine $S_{17}(0)$, the astrophysical S factor of the long-studied ^{7}Be(p,γ)^{8}B reaction at solar energies [3]. This method relies on the very peripheral character of this capture process at solar energies. It consists in extracting nuclear quantities called Asymptotic Normalization Coefficients (ANC) from peripheral transfer cross-sections, through a Distorted Wave Born Approximation (DWBA) analysis. Knowing these quantities, the S factor of the capture reaction can then be reliably calculated.

From the experimental point of view, the obvious advantage of such method lies in the cross-section magnitudes, which allow to make a measurement within a few days with secondary beams nowadays available. So far, this method (to which we shall refer as the ANC method) has only been applied to the above mentioned ^{7}Be(p,γ)^{8}B solar reaction [4–6], and also to some test cases, the ^{16}O(p,γ)^{17}F [7] and the ^{12}C(n,γ)$^{13}C^*$ [8] reactions. For these two test cases the S factors obtained from the ANC method were found in good agreement with those extracted from a direct capture measurement.

In this letter, we report on an experimental study of the ^{8}B(d,n)^{9}C proton transfer reaction from which the S factor of the ^{8}B(p,γ)^{9}C capture reaction can be derived using the ANC method. The ^{8}B(p,γ)^{9}C capture at astrophysical energies represents a case similar to the ^{7}Be(p,γ)^{8}B reaction, predicted to be non-resonant (direct) and strongly dominated by an electric dipole (E1) transition in the energy range of interest [9]. Nevertheless, the peripheral character of the capture is expected to be less pronounced than for the former reaction, due to the larger proton separation energy in ^{9}C, 1.256 MeV instead of 0.137 MeV in ^{8}B.

The ^{8}B(p,γ)^{9}C is of interest for the nucleosynthesis in stars (such as supermassive stars [10]) where temperatures and densities are such that it can compete with the β decay of ^{8}B, becoming a possible alternative path to the synthesis of CNO elements (the so-called hot proton-proton chain). A recent calculation

of the S factor for this reaction (which we will note S_{18}) was performed [9] and the result was found to be in disagreement with a previous evaluation [10]. On the experimental side, only a preliminary estimate was determined from a Coulomb dissociation measurement of ^{9}C [11]. This estimate was found to be consistent with the prediction of [9], but smaller by a factor three to four than the calculated value of [10].

2 Experiment and results

The experiment was performed at the RIKEN Accelerator Research Facility where we have measured the cross-section of the ^{8}B(d,n)^{9}C reaction at 14.4 MeV/u. The ^{7}Be(d,n)^{8}B cross-section was also measured in the same run but in this Letter, we restrict ourselves to the results obtained for the former reaction.

The radioactive ^{8}B beam was produced by fragmentation of a 70 A·MeV ^{12}C primary beam, using the RIPS [12] fragment separator. As mentioned above, a relatively low incident energy is required in order to fulfill the condition of peripherality. Using a thick ^{9}Be target (1.2 g/cm^2) and an aluminum achromatic wedge (mean thickness = 400 mg/cm^2), the ^{8}B yield was roughly 10^4 s^{-1} at the energy of 14.4 MeV/u. The momentum acceptance was set using slits placed at the dispersive focal plane (F1) of RIPS, in order to obtain an energy spread of $\pm 2\%$. Although ^{7}Be fragments represented most of the secondary beam produced, the incident ^{8}B particles was identified unambiguously event-by-event, by measuring the time of flight(TOF) between the two last focal planes of RIPS (F2 and F3). This was achieved by means of parallel plate avalanche counters (PPAC) capable of accepting count rates up to a few times 10^5/s.

The transfer reaction itself was studied at the final focal point F3 of RIPS. Upstream of the reaction target, a set of two position sensitive PPAC's provided a determination of the (X,Y) positions in the plane perpendicular to the beam, allowing to deduce incident position and angle. The beam spot size at the target position was 2cmx2cm FWHM. The deuteron target consisted of deuterated polyethylene (CD2) foils of relatively large size (5cmx8cm), the total thickness being 5.7 mg/cm^2. The ejectile detection system was composed of three thin plastic scintillators, placed at 38cm downstream of the target. The first two detectors, 0.25mm thick, were used as ΔE-E telescope for ^{9}C ejectile identification. The last detector (1mm thick) served as a veto detector to reject beam particles, whose range in plastic was much larger than for the ejectiles which stopped in the second detector. This latter point was carefully checked by tuning RIPS in order to produce ^{9}C of the same energy as the ejectiles, and then check their range. Position dependence of the signals were

checked by use of a PPAC with sensitive area of 15cm (H) X 10 cm (V) placed right before the plastic detectors. Finally, recoiling neutrons were detected in coincidence with ejectiles by eight cylindrical plastic BC408 scintillators cells, 14cm diameter and 3.81cm thick, coupled to a phototube through a conical light guide. They were placed at backward angles with respect to the beam direction (corresponding to forward angles in the center of mass (CM)), covering individually a solid angle of 20 msr in the laboratory frame.

Figure 1 shows the excitation energy spectrum obtained from the neutron TOF and angle in coincidence with ^{9}C ejectiles. The statistics are rather low, but the peak corresponding to the population of the ground state shows up very clearly. Counts at negative excitation energy correspond to random coincidences. The counts at excitation energies greater than zero correspond to the sum of random coincidences and to background neutrons having larger TOF than the neutrons from the ground state, mainly originating from scattering on beam pipe and chambers. These counts do not correspond to excited states in ^{9}C since only the ground state of this nucleus is bound and events in Figure 1 are gated on ^{9}C ejectiles. In the following, random coincidences will be substracted for the cross-section determination.

For absolute normalization of cross-sections, a precise determination of the neutron detection efficiency is necessary. We measured this efficiency during a separate run at the Orsay tandem accelerator, by studying the p(^{7}Li,^{7}Be)n reaction at 40 MeV, which produces neutrons in the energy range of interest (2-4 MeV). With this method, sometimes referred to as the associated particle technique [14], the absolute counting efficiency of the detectors is simply the ratio between ^{7}Be events in coincidence with neutrons to the number of ^{7}Be single events. It has to be noted that for the present neutron energy range, the efficiency is nearly independent of the threshold adjustment provided that this threshold is fixed sufficiently low (about 60 keV electron-equivalent energy in our case). The deduced error on the neutron efficiency was 8%. The total thickness and homogeneity of the CD2 target were determined during a separate run at the Orsay tandem accelerator, via the measurement of p-d elastic scattering at 22 MeV, for which the cross-section is accurately known [13]. The error on the target thickness deduced from this analysis was 6%. Finally, the uncertainty on the number of incident particles was considered as negligible since they were recorded on tape with a fixed sample rate during each run.

3 DWBA Analysis

The spin and parity values of ^{8}B and ^{9}C are respectively 2^{+} and $3/2^{-}$. Two components contribute to the ^{8}B(d,n)^{9}C cross-section, corresponding to ($l = 1, j = 3/2$) and ($l = 1, j = 1/2$) transfers. When the reaction is periph-

eral, transfer cross-sections can be factorized in terms of ANC's instead of spectroscopic factors. These ANC's can then be determined by normalizing DWBA cross-sections to the data , but without the large uncertainties inherent to spectroscopic factors due to the ambiguities on the potential parameters used to calculate the form factors [2]. The experimental cross-section for the ^{8}B(d,n)^{9}C reaction can be written as [15]:

$$\sigma(\theta) = (C_{1,3/2})^2 \frac{\sigma_{1,3/2}(\theta)}{b^2_{1,3/2}} + (C_{1,1/2})^2 \frac{\sigma_{1,1/2}(\theta)}{b^2_{1,1/2}} \quad (1)$$

where $\sigma_{l,j}$ are the calculated DWBA cross-sections (including the spin-statistical factors), and $b^2_{l,j}$ are given by the ratio $(u_{lj}(r)/W^+(r))^2$ at large radius , $u_{lj}(r)$ being the single-particle wave functions used in the DWBA calculation as form factors, and $W^+(r)$ the Whittaker function. In the asymptotic region, $b^2_{l,j}$ is constant and represents the squared amplitude of the tail of the single-particle wave-function. $C_{1,3/2}$ and $C_{1,1/2}$ are the two ANC's for the virtual decay ^{9}C $\rightarrow$ ^{8}B + p, from which the S factor of the ^{8}B(p,γ)^{9}C reaction can be extracted.

DWBA cross sections $\sigma_{l,j}$ were calculated using the zero-range code DWUCK4 [16] with a (d,n) normalization factor of 1.58 [17] . These calculations were performed without finite-range and non-locality corrections. Full finite-range calculations were also performed using the code DWUCK5 [18] and including the effect of the deuteron d-state. The obtained results are consistent with those of zero-range calculations within less than 8%, a variation distinctly smaller than the uncertainty due to the choice of the optical potential or to the statistical error as will appear later. The proton bound-state wave functions were determined by adjusting the well-depth of a Woods-Saxon potential with "standard" parameters (radius $r_0 = 1.25$ fm, diffuseness $a = 0.65$ fm) and a spin-orbit Thomas term with $\lambda = 25$. The shapes of the angular distributions for $j = 3/2$ and $j = 1/2$ are similar, so that the relative contribution of both transitions cannot be determined from our data. In our case however, the ratio $\sigma_{l,j}/b^2_{l,j}$ is almost independent of j within $\pm 1\%$ accuracy (for $\theta_{CM} \leq 15^0$), due to the peripherality of the reaction studied as will be discussed at the end of the present section. Consequently, Eq. (1) can be written as:

$$\sigma(\theta) = ((C_{1,3/2})^2 + (C_{1,1/2})^2) \frac{\sigma_{1,3/2}(\theta)}{b^2_{1,3/2}} \equiv \mathcal{S}\sigma_{1,3/2}(\theta) \quad (2)$$

As in the case of the ^{7}Be(p,γ)^{8}B reaction [5], the sum $(C_{1,3/2})^2 + (C_{1,1/2})^2$ determines the overall normalization of the capture cross-section at astrophysical energies. It can be extracted by normalizing $\sigma_{1,3/2}$ to the transfer data. $\mathcal{S}$ is the spectroscopic factor which we discuss below.

Optical potentials to be used in DWBA calculations play a central role in the discussion of the accuracy of the ANC method. Since no elastic scattering data exists for either the entrance or exit channels, we have used sets of optical potentials for deuterons [19,20] and neutrons [21–24] derived from global formulae. The deuteron potential D2 [20] has been extensively used for stripping reactions, while the potential D1 [19] is more recent and was deduced from a broader set of data. For neutrons, potentials N1 and N2 of refs. [21] and [22], respectively, have been derived from a specific study of p-shell nuclei (at relatively low energy for the latter, however). Neutron potentials N3 [23] and N4 [24] were used for comparison.

Figure 2 shows the calculated angular distributions $\sigma_{1,3/2}$ using combinations of the optical potentials mentioned above, each curve being normalized to the plotted data points. All shapes are rather similar, and the poor statistics of the data does not allow to discriminate between the different curves. But these forward angle data points can be used to determine the normalization factor of the curves (the quantities of interest) with nearly 20% statistical uncertainty. The obtained values of $(C_{1,3/2})^2+(C_{1,1/2})^2$ using above combinations of optical potentials are plotted in table 1. These values exhibit fluctuations of about $\pm 19\%$ around the average value. In the calculation of S_{18} presented below, the average over all the plotted values of $(C_{1,3/2})^2 + (C_{1,1/2})^2$ has been used. As stressed in ref. [25] the determination of optical potentials, particularly in the entrance channel would significantly reduce the uncertainty on the ANC's. The uncertainties due to core deformation/excitation effects and to multistep processes are comparatively smaller.

The factorization of ANC's as expressed in Eq. (1) assumes that the reaction is peripheral enough to ensure that the cross-section is nearly proportional to the squared amplitude of the *tail* of the bound-state wave functions. This assumption can be checked by varying the potential parameters used to calculate the bound-state wave functions $u_{lj}(r)$ (thus changing the tail amplitude), and examining whether the ratio between the tail amplitude b^2 (with respect to the Whittaker function) and the (forward) cross-section remains constant. This ratio is presented in Table 2 for three different sets of Woods-Saxon binding potential parameters. These calculations use optical potential sets D1-N4 but other potentials lead to similar results. One observes that, while the cross-section varies relatively strongly with the form-factor parameters the ratio remains nearly constant (within 10%), thus providing an indication that the reaction studied is essentially peripheral.

As stressed in ref. [1,2], spectroscopic factors are more uncertain quantities than ANC's because of their larger dependence on the Woods Saxon used to calculate the proton form factor parameters. The experimental spectroscopic factor $\mathcal{S}$ deduced from Eq. (1) can still be compared to the predictions of the shell-model. The average value obtained by normalizing the calculated

DWBA cross-sections of fig.2 to the data is $\mathcal{S} = 0.73$. For comparison, shell-model calculations of the ^{9}C ground state were performed using successively Cohen-Kurath, Warburton and WBT (in a $p + sd$ model space) interactions. All three sets of calculations predict the spectroscopic factor $\mathcal{S}_{1,1/2}$ for the $p_{1/2}$ orbital to be less than 5% of the one for the $p_{3/2}$ orbital, $\mathcal{S}_{1,3/2}$. The sum of the corresponding spectroscopic factors $\mathcal{S}_{1,3/2} + \mathcal{S}_{1,1/2} \approx \mathcal{S}$ ranges in the interval $0.81 - 0.97$, slightly above but close to the experimentally determined value of 0.73. Such values are substantially lower than the one calculated in ref. [10] ($\mathcal{S} = 2.5$). In their calculation, the authors performed a rough estimate of the spectroscopic factor by restricting themselves to the ^{6}Li-core plus three protons in the $1p_{3/2}$ orbital (neglecting configuration mixing), thus getting a large value of $\mathcal{S}$.

4 Calculation of S_{18} from the ANC's

The astrophysical S factor S_{18} can be deduced from the ANC's by calculating the matrix elements for the electromagnetic transition induced by the capture process. We have already mentioned that in the present case (just as in the case of the calculation of S_{17}), the largely dominant contribution to the transition is of electric dipole character. In a potential model, the matrix elements for E1 transitions are:

$$Q_{c\to b}^{(\mathrm{E1})} = < \Psi_c \mid\mid \hat{T}^{\mathrm{E1}} \mid\mid \Phi_b > \tag{3}$$

where we have indicated with subscript c the proton in the continuum (scattering channel) and with b the bound-state, here corresponding to the ^{9}C ground state. The capture cross section is simply given by

$$\sigma_{c\to b}^{(\mathrm{E1})}(p,\gamma) = \frac{16\pi}{9}\frac{k_\gamma^3}{\hbar v}\bar{e}^2 \sum_{c,b} \mid Q_{c\to b}^{(\mathrm{E1})} \mid^2 \tag{4}$$

where the sum runs over the $\mathrm{s}_{1/2}$ and $\mathrm{d}_{3/2}$ components of the continuum connected with E1 transitions to the ^{9}C ground-state ($j^\pi = 3/2^-$). Here, $k_\gamma = \epsilon_\gamma/\hbar c$ is the photon wave number corresponding to a transition energy ϵ_γ, v the core-proton relative velocity in the continuum and $\bar{e}$ is the single-particle proton effective charge. The S factor is related to the proton capture cross section by the relation:

$$S_{18}(E) \equiv \sigma_{p,\gamma}(E)\, E\, e^{2\pi\eta} \tag{5}$$

where E is the proton-^{8}B relative energy and $\eta = Ze^2/\hbar v$ is the Sommerfeld parameter. When the capture is peripheral, the radial component of Φ_b in the

asymptotic region can be written as:

$$u_{lj}(r) \approx b_{lj} W^{+}_{\eta,l}(k_b r) \tag{6}$$

where b_{lj} are the constants defined in the previous section, $W^{+}_{\eta,l}$ the Whittaker function and k_b the bound-state proton wave number. Therefore, the matrix elements are proportional to the ANC's and the sum $(C_{1,3/2})^2+(C_{1,1/2})^2$ defines the absolute normalization of the capture cross-section.

The approximation represented by Eq. (6) is correct provided that the major contribution to the E1 matrix elements is from the *asymptotic* region. In general, this must be checked case by case when one wants to apply the ANC method to determine capture cross-sections. It can be investigated in the same way as in the transfer case, namely by checking the proportionality between the capture cross-section (or the S factor S_{18}) and the amplitude of the tail of the bound-state. For that purpose, one can vary the potential parameters used to calculate the wave functions Φ_c and Φ_b, which was done using the same potential parameters as in the case of the transfer (set 1-3 of table 1). The ratio between S_{18} and b^2, the tail amplitude, was found to be constant within nearly 10% at 1 keV CM energy, as can be seen in table 1. One can conclude that the ^{8}B(p,γ)^{9}C reaction, although less peripheral than ^{7}Be(p,γ)^{8}B at astrophysical energies, can be investigated using the ANC technique since the main contribution to the capture comes from the large radius region. At higher CM energies (above a few hundred keV) the interior starts playing an important role, the above approximations no longer hold, and the potential model becomes too uncertain.

The energy dependence of S_{18} deduced from the model presented above in the CM energy range 1-100 keV is a slow decrease by nearly 3%. In this energy domain, the average value is $S_{18} = 45 eV.b$. The estimated error due to the contribution of errors on the neutron detector efficiency(8%), absolute thickness of the target(6%), the choice of the optical potential in the DWBA calculation (19%) and the statistical error(20%) is $\pm 13 eV.b$. Our result on S_{18} is roughly a factor of two lower than the calculated value reported in [9] (about 85 eV.b), where a microscopic cluster description of the ^{9}C structure was used. Such tendency of microscopic cluster models to overestimate absolute cross-sections was already observed in the case of S_{17}, the S-factor of the ^{7}Be(p,γ)^{8}B reaction at solar energies. Values of $S_{17}(0)$ deduced by similar calculations as in [9] stand near 27-30 eV.b depending on the interaction used, while the currently adopted value is 19^{+4}_{-2} eV.b [3]. In ref. [10], the mean value of S_{18}, averaged over the energy range $E_p \leq 0.8 MeV$ was found to be $S_{18} \approx 210 eV.b$, much higher than our results. The origin of such large value certainly comes from the value of 2.5 for the spectroscopic factor, well above both the one extracted from the present data, and those estimated in our shell model calculations.

In conclusion, we have provided for the first time an experimental determination of the S factor of the ^{8}B(p,γ)^{9}C reaction by applying the ANC technique, particularly suitable in this case where short-lived nuclei are involved. Our result is lower by nearly a factor two than the one predicted in recent microscopic calculations.

We wish to thank the RIKEN RARF and Orsay tandem accelerator staffs. We acknowledge Dr. N. Smirnova for shell-model calculations, and Dr. Y. Blumenfeld, Dr. S. Galès and Dr. J.P. Thibaud for careful reading of the manuscript. Part of this work was achieved within the IN2P3-RIKEN agreements and supported by the Science and Technology Agency of the Japanese government.

References

[1] H.M. Xu *et al.*, Phys. Rev. Lett. 73 (1994) 2027.

[2] A. M. Mukhamedzhanov, R.E. Tribble and N.K. Timofeyuk, Phys. Rev. C 51 (1995) 3472.

[3] E.G. Adelberger *et al.*, Rev. Mod. Phys. 70 (1998) 1265 and references therein.

[4] W. Liu *et al.*, Phys. Rev. Lett. 77 (1996) 611.

[5] A. Azhari *et al.*, Phys. Rev. Lett. 82 (1999) 3960.

[6] A. Azhari *et al.*, Phys. Rev. C 60 (1999) 055803.

[7] C.A. Gagliardi *et al.*, Phys. Rev. C 59 (1999) 1149.

[8] N. Imai *et al.*, proc. of the "Nuclei in the Cosmos 2000" conference, to be published.

[9] P. Descouvemont, Nucl. Phys. A 646 (1999) 261.

[10] M. Wiescher *et al.*, Astrophys. J 343 (1989) 352.

[11] T. Motobayashi in ENAM 98 : Exotic Nuclei and Atomic Masses, edited by B.M. Sherrill, D.J. Morrissey and C.N. Davids, AIP Conf. Proc. No.455(AIP, New York, 1998), p.882; I. Hisanaga et al., to be submitted.

[12] T. Kubo *et al.*, Nucl. Instrum. Methods B 70 (1992) 309.

[13] S.N. Bunker *et al.*, Nucl. Phys. A 113 (1968) 461.

[14] G. Guillaume *et al.*, Nucl. Instrum. Methods Phys. Res. A 277 (1989) 458.

[15] A. M. Mukhamedzhanov *et al.*, Phys. Rev. C 56 (1997) 1302.

[16] P.D. Kunz, code DWUCK4, University of Colorado (unpublished)

[17] G.R. Satchler, Direct Nuclear Reactions, Oxford University Press, 1983, chap.17

[18] P.D. Kunz, code DWUCK5, University of Colorado (unpublished)

[19] W.W. Daehnick, J.D. Childs and Z. Vrcelj, Phys. Rev. C 21 (1980) 2253.

[20] C.M. Perey and F.G. Perey, Phys. Rev. 132 (1963) 755.

[21] B.A. Watson, P.P. Singh, R.E. Segel, Phys. Rev. 182 (1969) 977.

[22] J.H. Dave and C.R. Gould, Phys. Rev. C 28 (1983) 2212.

[23] D. Wilmore and P.E. Hodgson, Nucl. Phys. 55 (1964) 673.

[24] F.D. Becchetti and G.W. Greenlees, Phys. Rev. 182 (1969) 1190.

[25] J.C. Fernandes, R. Crespo, F.M. Nunes and I.J. Thompson, Phys. Rev. C 59 (1999) 2865.

Figure captions

Figure 1. Excitation energy spectrum in ^{9}C deduced from neutron angle and time-of-flight.

Figure 2. Angular distribution of the ^{8}B(d,n)^{9}C reaction at 14.4 MeV/u compared with DWBA calculations using different sets of optical potentials. D1 and D2 correspond to the optical potentials for d+^{8}B from refs. [19] and [20], respectively. Optical potentials N1,N2,N3,N4 for n+^{9}C are from [21], [22], [23], [24], respectively. All curves have been normalized to the data.

optical potentials	$(C_{1,3/2})^2 + (C_{1,1/2})^2$ [fm^{-1}]
D1-N1	0.97
D1-N2	1.11
D1-N3	1.15
D1-N4	1.11
D2-N1	1.17
D2-N2	1.42
D2-N3	1.22
D2-N4	1.30

Table 1

Values of the sum of squared ANC's $(C_{1,3/2})^2+(C_{1,1/2})^2$ deduced from the ^{8}B(d,n)^{9}C cross-section at 14.4 MeV/u by using combinations of optical potentials in the entrance and exit channels. D1 and D2 correspond to the optical potentials for d+^{8}B from refs. [19] and [20], respectively. Optical potentials N1,N2,N3,N4 for n+^{9}C are from [21], [22], [23], [24], respectively.

set	V_0 (MeV)	r_0 (fm)	a (fm)	$\sigma^{DWBA}(6^o)$ (mb/sr)	$b^2/\sigma^{DWBA}(6^o)$	S_{18} (eV.b)	b^2/S_{18}
1	44.4	1.25	0.65	6.01	0.269	61.5	0.274
2	65.6	0.95	0.65	4.63	0.259	48.1	0.253
3	39.4	1.35	0.45	4.85	0.275	48.7	0.279

Table 2

The potential parameters used to calculate the bound-state wave function, and the corresponding ratios of the squared tail amplitude of these wave functions to the calculated transfer cross-section at 6^o in the center of mass, and to the S-factor S_{18} at 1 keV CM energy.

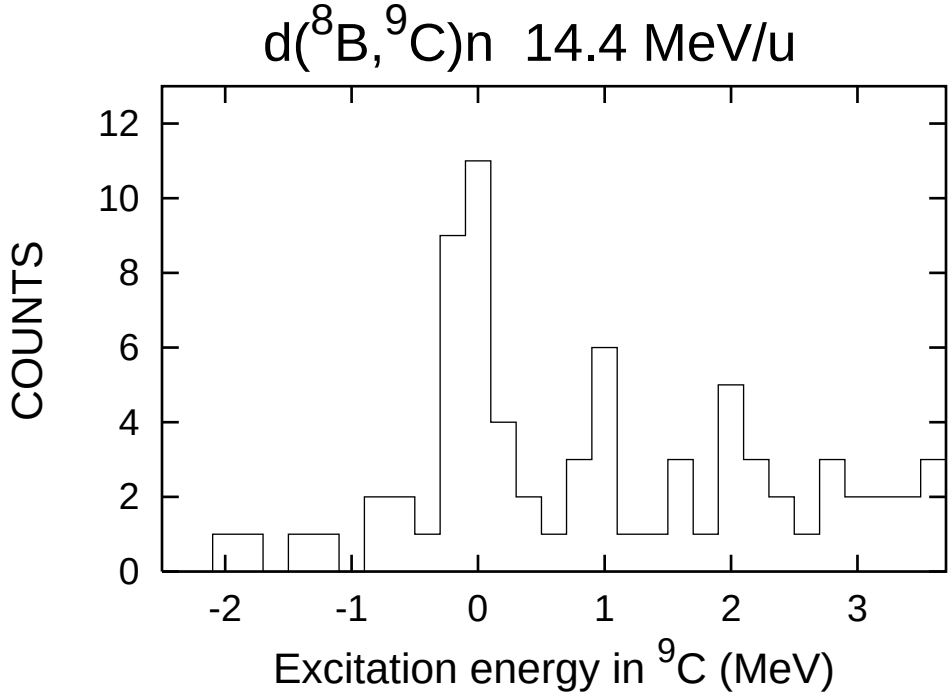

Fig. 1. Excitation energy spectrum in ^{9}C deduced from neutron angle and time-of-flight.

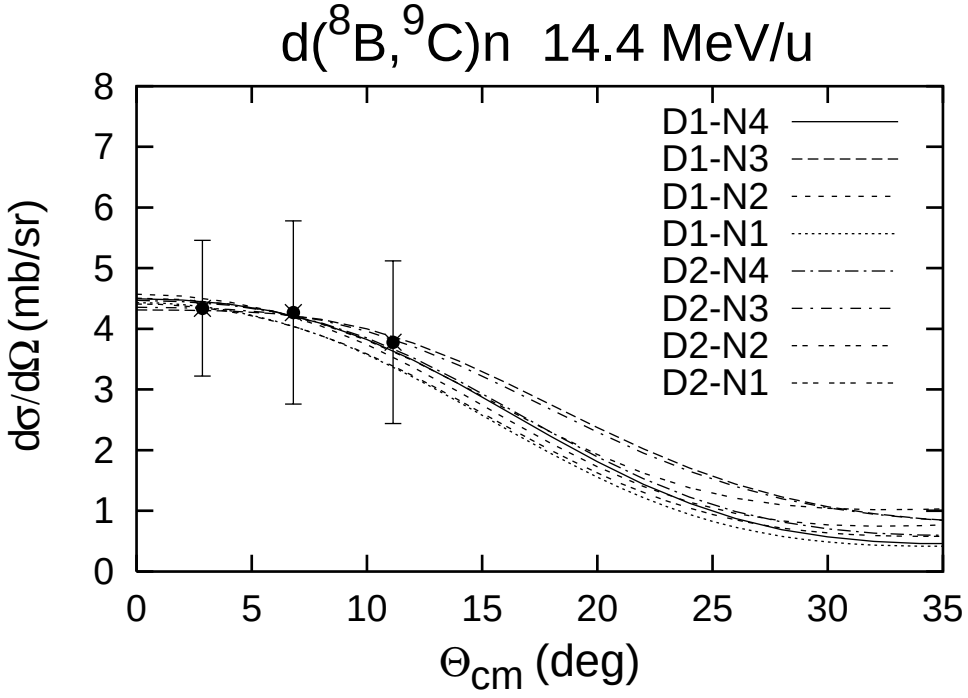

Fig. 2. Angular distribution of the ^{8}B(d,n)^{9}C reaction at 14.4 MeV/u compared with DWBA calculations using different sets of optical potentials. D1 and D2 correspond to the optical potentials for d+^{8}B from refs. [19] and [20], respectively. Optical potentials N1,N2,N3,N4 for n+^{9}C are from [21], [22], [23], [24], respectively. All curves have been normalized to the data.